

Absence of electron-phonon-mediated superconductivity in hydrogen-intercalated nickelatesSimone Di Cataldo^{1,*}, Paul Worm,¹ Liang Si,² and Karsten Held¹¹*Institut für Festkörperphysik, Technische Universität Wien, 1040 Wien, Austria*²*School of Physics, Northwest University, Xi'an 710127, China*

(Received 7 April 2023; accepted 31 October 2023; published 22 November 2023)

A recent experiment [X. Ding *et al.*, *Nature (London)* **615**, 50 (2023)] indicates that superconductivity in nickelates is restricted to a narrow window of hydrogen concentration, $0.22 < x < 0.28$ in $\text{Nd}_{0.8}\text{Sr}_{0.2}\text{NiO}_2\text{H}_x$. This reported necessity of hydrogen suggests that it plays a crucial role for superconductivity, as it does in the vast field of hydride superconductors. Using density-functional theory and its extensions, we explore the effect of topotactic hydrogen on the electronic structure and phonon-mediated superconductivity in nickelate superconductors. Our calculations show that the electron-phonon coupling in hydrogen-intercalated nickelates is not strong enough to drive the electron pairing, and thus cannot explain the reported superconductivity.

DOI: [10.1103/PhysRevB.108.174512](https://doi.org/10.1103/PhysRevB.108.174512)**I. INTRODUCTION**

Our understanding of the pairing mechanism and gap function in the recently synthesized nickelate superconductors [1–6] is still in its infancy, and it goes without saying that it is controversially debated. Scanning tunneling microscopy (STM) shows both a U and a V shape gap [7], depending on the precise position of the tip on the surface and indicative of a d - and s -wave gap, respectively. Fits to the London penetration depth either point to a nodeless [8] or a nodal [9] gap.

Theories range from d -wave superconductivity originating from spin fluctuations in the Ni $d_{x^2-y^2}$ orbital [10–13] to two-orbital physics with d - and s_{\pm} -wave superconductivity [14]. Also superconductivity based on a Kondo coupling between Ni spin and Nd bands [15], the importance of the interorbital Coulomb interaction [16], and a possible connection to charge ordering [17] have been suggested, among others.

Early calculations [18,19] indicated that topotactic hydrogen might be intercalated when reducing $\text{Nd}_{0.8}\text{Sr}_{0.2}\text{NiO}_3$ to $\text{Nd}_{0.8}\text{Sr}_{0.2}\text{NiO}_2$ with the reagent CaH_2 [20]. The presence of hydrogen in nickelates has by now been established using nuclear magnetic resonance (NMR) [21] in film samples and using neutron scattering [22] in bulk LaNiO_2 , where H appears to cluster at the grain boundaries.

The work by Ding *et al.* [23] now prompts for a complete overhaul of our picture of superconductivity in nickelates. Systematically increasing the exposure time to CaH_2 and using ion mass spectroscopy, Ding *et al.* link the occurrence of superconductivity to a narrow range of hydrogen concentration $0.22 < x < 0.28$. Most notably, superconductivity seems absent for low hydrogen concentrations, implying that its presence is necessary for superconductivity. Arguably the most obvious—but hitherto for nickelates unexplored—route for hydrogen to cause superconductivity is via the

conventional, electron-phonon (e - p) mechanism. Due to its light mass, hydrogen can lead to high-temperature superconductivity, with critical temperatures (T_c) up to almost room temperature in hydrides under pressure [24–28]. Furthermore, the s -wave gap reported in Ref. [14] might be naturally explained from such an e - p mechanism. In this context, a hydrogen e - p mechanism for at least some of the superconductivity in nickelates appears to be a very reasonable and appealing working hypothesis. Let us also note that the e - p mechanism for nickelate superconductors without hydrogen has been explored previously, but does not result in sizable T_c 's at the density-functional theory (DFT) level [29].

In this paper, we thus explore the hydrogen e - p scenario for $\text{Nd}_{0.75}\text{Sr}_{0.25}\text{NiO}_2\text{H}_{0.25}$ which is exactly at the optimum of Ding *et al.* [23]. Since it is energetically favorable for hydrogen to form chains [18,30], the simplest structure compatible with the experimental observation is one hydrogen (chain) in a $2 \times 2 \times 1$ supercell (see Fig. 1). This supercell can also accommodate 25% Sr doping, close to the experimentally investigated 20% and still in the range of the superconducting dome [1,3,31]. We investigated the electronic and vibrational properties by means of DFT [32] and density-functional perturbation theory (DFPT) [33], respectively. We find however that the e – p coupling is minimal, and cannot explain the reported T_c 's. Furthermore, engineering optimal conditions for e - p superconductivity by changing the rare earth to La and performing a comprehensive study of different hydrogen concentrations does not yield any finite transition temperature either. We thus conclude that the measured T_c eludes an explanation in terms of a simple boost in the e - p coupling driven by hydrogen.

II. METHODS**A. DFT**

All DFT calculations were performed using QUANTUM ESPRESSO version 7.1, employing optimized norm-conserving Vanderbilt pseudopotentials [34,35]. The pseudopotential of

*simone.cataldo@tuwien.ac.at

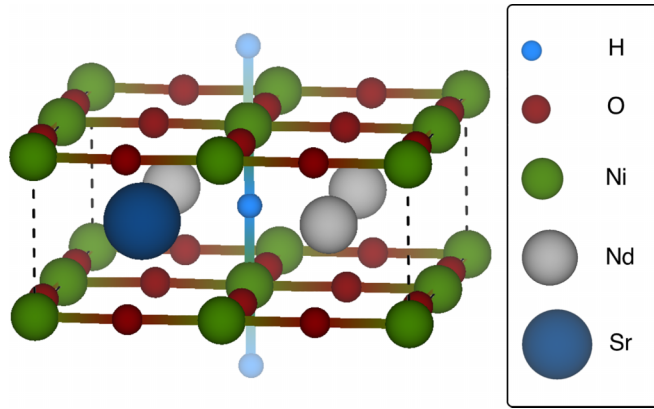


FIG. 1. A $2 \times 2 \times 1$ supercell for $\text{Nd}_{0.75}\text{Sr}_{0.25}\text{NiO}_2\text{H}_{0.25}$ with the experimentally optimal hydrogen concentration [23]. The hydrogen chain is indicated by two additional H atoms outside the supercell; atoms at the surface, edge, and corner count by a factor of $1/2$, $1/4$, and $1/8$, respectively.

neodymium uses the frozen-core approximation for the f states. We used a 90 Ry cutoff on the plane-wave expansion, and an $8 \times 8 \times 8$ grid with a 0.040 Ry smearing for Brillouin zone integration. The crystal structures were constructed using VESTA [36] and subsequently relaxed until forces (stresses) were lower than 10^{-5} Ry/bohr (0.5 kbar). Due to the larger size of Sr compared to Nd a local distortion of the Ni-O-Ni bond angle is induced, which deviates from 180° to 172° around Sr to accommodate the atom; see Supplemental Material Fig. S1 [37] (see also Refs. [34–36,38–41] therein).

Phonon calculations were performed on a Γ -centered $2 \times 2 \times 2$ grid, within the harmonic approximation. Anharmonic corrections were introduced for specific modes using the frozen-phonon approach presented in Ref. [41] (further details are available in the Supplemental Material [37]). The integral of the electron-phonon matrix elements was performed on a $16 \times 16 \times 16$ and $24 \times 24 \times 24$ grid. A Gaussian smearing of 100 meV was found to give a converged result. The rigid-band approximation for the integration of the e - p matrix elements was performed using our modified version of QUANTUM ESPRESSO (see Ref. [42]).

B. Superconductivity

In a conventional e - p superconductor the superconducting T_c can be estimated by the McMillan formula [40,43], which works particularly well in the weak-coupling regime,

$$T_c = \frac{\omega_{\log}}{1.2} \exp\left[-\frac{1.04(1+\lambda)}{\lambda - \mu^*(1+0.62\lambda)}\right], \quad (1)$$

where λ and ω_{\log} describe the average strength of the e - p coupling and phonon energies, respectively. It is apparent from Eq. (1) that high T_c 's require a combination of both (i) strong e - p coupling (large λ) and (ii) high phonon energy (large ω_{\log}). Generally speaking, hydrogen can boost both of these quantities as phonons involving it are typically high energy and unscreened, and hydrogen-rich conventional superconductors have indeed reached extremely high T_c 's [24–28].

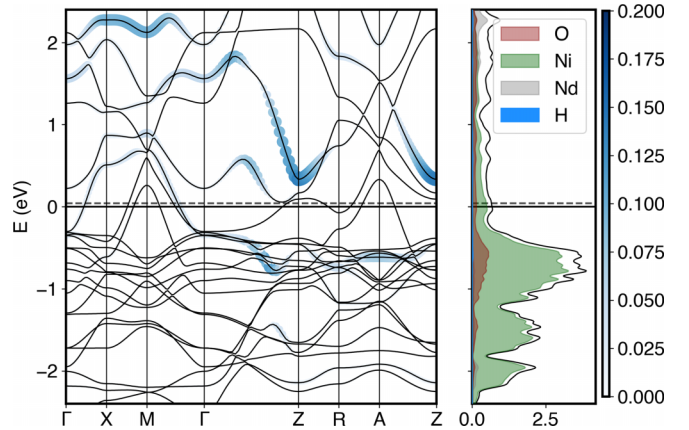


FIG. 2. Left: Electronic band structure of $\text{Nd}_{0.75}\text{Sr}_{0.25}\text{NiO}_2\text{H}_{0.25}$, decorated with the orbital projection onto the H $1s$ state. Right: Total and atom-projected density of states. The size and color scale of the colored bands (left) indicates the H fraction of states, from 0 (light blue) to 0.20 (dark blue). The Fermi energy for 25% and 20% Sr doping is shown as a solid black and dashed gray line, respectively. The DOS (right) is in units of states/eV/f.u. The atom projection onto Nd(+Sr), Ni, O, and H is shown as gray, green, red, and blue solid curves, respectively.

Fermi-surface nesting for $\text{Nd}_{0.75}\text{Sr}_{0.25}\text{NiO}_2\text{H}_{0.25}$ was computed using the EPW code [39,44], with a Wannier interpolation over a $32 \times 32 \times 32$ grid (for further details on the Wannierization we refer the reader to the Supplemental Material [37]). In $\text{Nd}_{0.75}\text{Sr}_{0.25}\text{NiO}_2\text{H}_{0.25}$ EPW was also used to provide an additional convergence test of e - p properties by interpolating the e - p matrix elements over a $12 \times 12 \times 12$ and $24 \times 24 \times 24$ grid for phonons and electrons, respectively, still yielding a T_c of 0 K.

III. ELECTRONIC STRUCTURE

In Fig. 2 we show the electronic band structure (left) decorated with the hydrogen $1s$ character, and the orbital resolved density of states (right) of $\text{Nd}_{0.75}\text{Sr}_{0.25}\text{NiO}_2\text{H}_{0.25}$ (a comparison with the band structure of the parent compound $\text{Nd}_{0.75}\text{Sr}_{0.25}\text{NiO}_2$ is shown in the Supplemental Material [37] Fig. S2; it has also been calculated before, e.g., in Refs. [10,15,29,45]). The presence of topotactic hydrogen opens a wide gap around the Z point, slightly above the Fermi energy, and another one in the band going from Γ to Z. These bands can be identified easily since they present a significant hydrogen character. Due to its low concentration relative to the other elements, hydrogen contributes to only about 2% of the density of states (DOS) at the Fermi level. A band with significantly higher hydrogen character is present along the $\Gamma - Z$ direction, at about 0.5 eV above the Fermi energy, which is, however, too high to contribute significantly to superconductivity.

The Fermi surface consists of three sheets (shown in Supplemental Material [37] Fig. S3): a long, tubular sheet forming an electron pocket around Γ , and similar hole pockets around M , elongated along the k_z direction. None of these sheets presents a significant hydrogen character, which is rather evenly spread over all wave vectors.

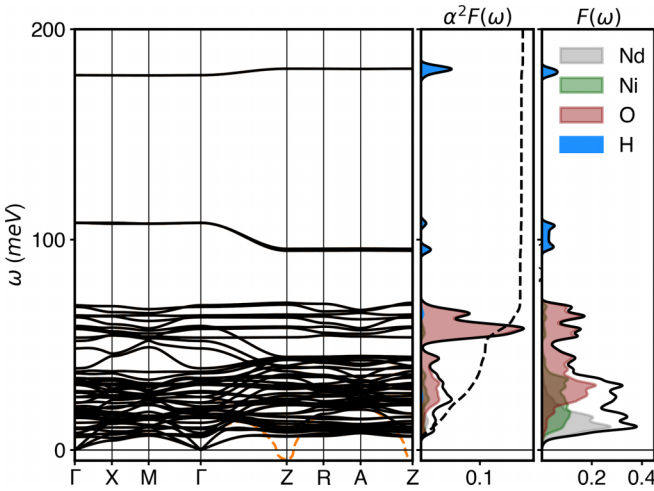


FIG. 3. Phonon dispersions (left), atom-projected Eliashberg function [$\alpha^2 F(\omega)$; middle], and phonon density of states [$F(\omega)$; right]. In the harmonic approximation, there is an instability at the Z point (orange dashed orange lines), which is removed when including the anharmonic correction at this point (black solid lines). The total phonon DOS and Eliashberg function are shown as black solid lines, while projections onto Nd(+Sr), Ni, O, and H are shown as gray, green, red, and blue solid curves.

IV. ELECTRON-PHONON SUPERCONDUCTIVITY

To establish whether the presence of hydrogen leads to a significant superconducting T_c via the conventional e - p mechanism, we computed the superconducting properties using DFPT as implemented in QUANTUM ESPRESSO [33,46,47]. In Fig. 3 we report the phonon dispersions along with the atom-projected phonon density of states and the Eliashberg function.

The phonon dispersion is characterized by two rather flat branches at about 110 and 180 meV, which correspond to the twofold-degenerate in-plane (Nd-H) and out-of-plane (Ni-H) hydrogen vibrations. In addition, a single mode involving in-plane bending of the Ni-O bond presents a small imaginary frequency at the Z point. Inclusion of anharmonic effects via a frozen-phonon approach as in Ref. [41] is enough to remove this instability, as the anharmonic mode goes from $6i$ to 9 meV [48]. Using the same approach, we computed the anharmonic vibrational frequency for the Ni-H and Nd-H modes at the Γ point. In the Ni-H mode, we observe a hardening of the mode from 178 to 191 meV, while for the Nd-H mode, we found the anharmonic frequency at 113 meV is only 5 meV higher than the harmonic result. To check the possible influence of anharmonicity on the e - p coupling, we diagonalized the dynamical matrix with the anharmonic frequency, and computed the coupling both with and without it, but found no significant change in our results.

The phonon modes involving Ni-H and Nd-H exhibit only an extremely small e - p coupling and thus essentially do not contribute to superconductivity. Indeed, the integrated e - p coupling and average phonon frequency are $\lambda = 0.16$ and $\omega_{\log} = 43.4$ meV, respectively. This means that the superconducting T_c estimated via the McMillan formula is essentially zero ($\mu^* = 0.10$) [40,43], and the T_c observed in Ref. [23]

TABLE I. Summary of the calculated superconducting properties of various nickelate compounds with topotactic hydrogen.

Composition	λ	ω_{\log} (meV)	T_c (K) ^a
Nd _{0.75} Sr _{0.25} NiO ₂ H _{0.25}	0.16	43.4	0
Nd _{0.80} Sr _{0.20} NiO ₂ H _{0.25} ^b	0.17	44.1	0
LaNiO ₂ H _{0.11}	0.21	33.0	0
LaNiO ₂ H _{0.22}	0.21	36.5	0
LaNiO ₂ H _{0.25}	0.21	42.8	0
LaNiO ₂ H _{0.55}	0.17	39.0	0

^aCalculated T_c 's below 1 mK are considered as zero. The T_c in the fourth column was computed using the formula in Eq. (1), using a value of the Morel-Anderson pseudopotential $\mu^* = 0.10$.

^bCalculated by shifting the Fermi energy.

cannot be explained. To further rule out the unlikely event that the small difference in doping between the experimental compound (Nd_{0.8}Sr_{0.2}NiO₂H_{0.25}) and our calculations (Nd_{0.75}Sr_{0.25}NiO₂H_{0.25}) induces a significant change in T_c , we performed the same calculations for an effective 20% Sr doping [49] using a rigid-band approximation. The results are summarized in Table I; both λ and ω_{\log} remain essentially identical and the resulting T_c is also zero.

V. ENGINEERING OPTIMAL CONDITIONS FOR e - p SUPERCONDUCTIVITY IN HYDROGENATED NICKELATES

In the previous section we discussed the absence of e - p mediated superconductivity in Nd_{0.75}Sr_{0.25}NiO₂H_{0.25}. However, as previously noted, a stronger hydrogen character is present at about 0.5 eV above the Fermi level (Fig. 2), which might move towards the Fermi energy given a slight modification in the crystal structure and/or a higher electron filling. Since in superconducting hydrides the hydrogen character of states at the Fermi energy typically correlates with higher T_c 's [50,51], this level of filling would appear more promising for the scenario of conventional superconductivity.

To explore this possibility and the effect of different rare-earth cations, we studied different hydrogen configurations of the closely related LaNiO₂H_x compound. Indeed, a hydrogen concentration of 25%, consistent with that reported in Ref. [23], yields an electronic structure that favors the previously outlined scenario. That is, the bands with the largest hydrogen character that are 0.5 eV above the Fermi level for NdNiO₂H_{0.25} are crossing the Fermi energy for LaNiO₂H_{0.25} (see Supplemental Material [37] Fig. S5). We thus computed the vibrational and superconducting properties for four different topotactic hydrogen concentrations $x = 11\%$, 22% , and 55% (in a $3 \times 3 \times 1$ supercell), and 25% (in a $2 \times 2 \times 1$ supercell) for LaNiO₂H_x. A summary of these results is shown in Table I. Despite the more favorable conditions for e - p mediated superconductivity, we find a total e - p coefficient λ no higher than 0.21 in all the configurations investigated. Thereby we confirm that, albeit the contribution of hydrogen can be slightly more significant, the e - p coupling remains low and cannot explain the observed T_c 's.

Our direct calculations of the e - p coupling thus show that the Ni-H or Nd/La-H bonds do not contribute sufficiently to

the e - p coupling to explain the T_c 's measured by Ref. [23]. In $\text{NdNiO}_2\text{H}_{0.25}$, the e - p mechanism is not particularly supported by the electronic structure, since no bands that cross the Fermi energy exhibit significant hydrogen character—an important ingredient for superconductivity in hydrides [50,52]. However, even when the hydrogen bands are located at the Fermi energy they do not cause a significant T_c . This is most likely due to the ionic character of the La-H and Ni-H bonds [53], which cause the e - p matrix elements to be small.

VI. ENHANCED T_c FROM FERMI-SURFACE NESTING

Having established that the electron-phonon matrix elements are in general small, the only other scenario supporting conventional superconductivity could come from an enhancement due to Fermi-surface nesting [41,54]. On a qualitative level, the squarelike sheet of the Fermi surface could indeed support this for phonons with wave vectors $\vec{q}_{\text{nest}} \sim (0.0, 0.4, 0.0)$ and $(0.4, 0.0, 0.0)$ [55].

To examine this possibility, we computed the Fermi-surface nesting function, defined as in Refs. [38,39], along a high-symmetry path (see Supplemental Material [37] Fig. S4), which presents two local maxima at X and M . Since these points were already present in the mesh used for the e - p calculations, we also rule out nesting as a possible source of elusive e - p interaction.

VII. CONCLUSION

We investigated the possibility of topotactic hydrogen inducing superconductivity in nickelates through the conventional electron-phonon mechanism. Experimentally Sr-doped nickelates with a T_c of about 15 K appear to be extremely sensitive to the hydrogen concentration and some experiments suggest an s -wave gap that is to be expected in this scenario. Notwithstanding, we find that hydrogen does not strongly affect the states at the Fermi surface and that the e - p coupling is too weak. The e - p mediated T_c of $\text{Nd}_{0.75}\text{Sr}_{0.25}\text{NiO}_2\text{H}_{0.25}$ is thus essentially zero.

To rule out that we missed the optimal conditions for e - p mediated superconductivity, we further engineered the band structure by changing the rare-earth atom and hydrogen concentration. This did not yield any finite T_c either. Given the very weak e - p coupling with $T_c < 1$ mK even under optimal conditions, we do not expect that many-body effects [18,56–59] beyond our DF(P)T calculation such as quasiparticle renormalization, Hund's exchange on Ni, and modifications of crystal-field splittings can enhance the T_c significantly. Consequently, we are inclined to conclude that hydrogen-derived phonons do not mediate superconductivity in infinite-layer nickelate superconductors.

Alternative explanations

So why does a narrow range of hydrogen concentration appear to be essential for superconductivity in nickelates? One possibility is that (i) the inclusion of hydrogen changes the electronic structure and environment in a manner that is favorable for a mechanism different from conventional e - p coupling. However, currently, none of the proposed mechanisms for superconductivity in infinite-layer nickelates relies on the presence of hydrogen. On the contrary, it has been argued [18,60] that the spin-1 state and three-dimensionality that is induced by topotactic hydrogen is unfavorable for superconductivity. Furthermore, it is at least somewhat unexpected that the window of hydrogen, where superconductivity is found, appears fairly small. With its agility, hydrogen will also tend to spread through the crystal and thus induce some disorder which is generally unfavorable for superconductivity.

Another possibility (ii) is that not only the hydrogen concentration is changed during the reduction process. Specifically, Ding *et al.* [23] use longer CaH_2 exposure times as a means to control the amount of intercalated H, and it is not unreasonable to surmise other aspects of the sample might alter as well. The most important is that these longer reduction times also affect the oxygen content which has to be reduced in the first place and which was not analyzed in Ref. [23]. The purported narrow range of hydrogen concentration might thus simply be the sweet spot of reduction time in $\text{Nd}_{0.8}\text{Sr}_{0.2}\text{NiO}_{2+\delta}\text{H}_x$ with δ already sufficient low but x not yet too high for superconductivity—and $\delta = x = 0$ being the unreachable optimum.

Note added. Recently, we became aware of a paper in which the measurement of a T_c of 80 K in the related compound $\text{La}_3\text{Ni}_2\text{O}_7$ was reported [61]. In this experiment no reduction with a hydride takes place, hence if confirmed, these results are further confirmation that superconductivity in nickelates is possible via an unconventional pairing.

Raw data and our modifications to QUANTUM ESPRESSO are available at the repository in Ref. [42].

ACKNOWLEDGMENTS

S.D.C. thanks Lilia Boeri for useful discussion, and Christoph Heil and Roman Lucrezi for sharing their code for calculating the anharmonic dynamical matrices. We acknowledge funding through the Austrian Science Funds (FWF) Projects ID I 5398, P 36213, SFB Q-M&S (FWF project ID F86), and Research Unit QUAST by the Deutsche Forschungsgemeinschaft (DFG; project ID FOR5249) and FWF (project ID I 5868). L.S. is thankful for the starting funds from Northwest University. Calculations have been done in part on the Vienna Scientific Cluster (VSC).

- [1] D. Li, K. Lee, B. Y. Wang, M. Osada, S. Crossley, H. R. Lee, Y. Cui, Y. Hikita, and H. Y. Hwang, Superconductivity in an infinite-layer nickelate, *Nature (London)* **572**, 624 (2019).
 [2] M. Osada, B. Y. Wang, K. Lee, D. Li, and H. Y. Hwang, Phase diagram of infinite layer praseodymium nickelate $\text{Pr}_{1-x}\text{Sr}_x\text{NiO}_2$ thin films, *Phys. Rev. Mater.* **4**, 121801(R) (2020).

- [3] S. Zeng, C. Li, L. E. Chow, Y. Cao, Z. Zhang, C. S. Tang, X. Yin, Z. S. Lim, J. Hu, P. Yang, and A. Ariando, Superconductivity in infinite-layer nickelate $\text{La}_{1-x}\text{Ca}_x\text{NiO}_2$ thin films, *Sci. Adv.* **8**, eabl9927 (2022).
 [4] M. Osada, B. Y. Wang, B. H. Goodge, S. P. Harvey, K. Lee, D. Li, L. F. Kourkoutis, and H. Y. Hwang, Nickelate

- superconductivity without rare-earth magnetism: (La, Sr)NiO₂, *Adv. Mater.* **33**, 2104083 (2021).
- [5] G. A. Pan, D. F. Segedin, H. LaBollita, Q. Song, E. M. Nica, B. H. Goodge, A. T. Pierce, S. Doyle, S. Novakov, D. C. Carrizales *et al.*, Superconductivity in a quintuple-layer square-planar nickelate, *Nat. Mater.* **21**, 160 (2022).
- [6] Let us also mention the preceding theoretical calculations suggesting the possibility of superconductivity in nickelate superconductors [62] and heterostructures thereof [63–65].
- [7] Q. Gu, Y. Li, S. Wan, H. Li, W. Guo, H. Yang, Q. Li, X. Zhu, X. Pan, Y. Nie, and H.-H. Wen, Single particle tunneling spectrum of superconducting Nd_{1-x}Sr_xNiO₂ thin films, *Nat. Commun.* **11**, 6027 (2020).
- [8] L. E. Chow, S. K. Sudheesh, P. Nandi, S. Zeng, Z. Zhang, X. Du, Z. S. Lim, E. E. Chia, and A. Ariando, Pairing symmetry in infinite-layer nickelate superconductor, [arXiv:2201.10038](https://arxiv.org/abs/2201.10038).
- [9] S. P. Harvey, B. Y. Wang, J. Fowlie, M. Osada, K. Lee, Y. Lee, D. Li, and H. Y. Hwang, Evidence for nodal superconductivity in infinite-layer nickelates, [arXiv:2201.12971](https://arxiv.org/abs/2201.12971).
- [10] X. Wu, D. Di Sante, T. Schwemmer, W. Hanke, H. Y. Hwang, S. Raghu, and R. Thomale, Robust $d_{x^2-y^2}$ -wave superconductivity of infinite-layer nickelates, *Phys. Rev. B* **101**, 060504(R) (2020).
- [11] M. Kitatani, L. Si, O. Janson, R. Arita, Z. Zhong, and K. Held, Nickelate superconductors—a renaissance of the one-band Hubbard model, *npj Quantum Mater.* **5**, 59 (2020).
- [12] M. Kitatani, L. Si, P. Worm, J. M. Tomczak, R. Arita, and K. Held, Optimizing superconductivity: From cuprates via nickelates to palladates, *Phys. Rev. Lett.* **130**, 166002 (2023).
- [13] J. Karp, A. Hampel, and A. J. Millis, Superconductivity and antiferromagnetism in NdNiO₂ and CaCuO₂: A cluster DMFT study, *Phys. Rev. B* **105**, 205131 (2022).
- [14] A. Kreisel, B. M. Andersen, A. T. Rømer, I. M. Eremin, and F. Lechermann, Superconducting instabilities in strongly correlated infinite-layer nickelates, *Phys. Rev. Lett.* **129**, 077002 (2022).
- [15] G.-M. Zhang, Y.-F. Yang, and F.-C. Zhang, Self-doped Mott insulator for parent compounds of nickelate superconductors, *Phys. Rev. B* **101**, 020501(R) (2020).
- [16] P. Adhikary, S. Bandyopadhyay, T. Das, I. Dasgupta, and T. Saha-Dasgupta, Orbital-selective superconductivity in a two-band model of infinite-layer nickelates, *Phys. Rev. B* **102**, 100501(R) (2020).
- [17] M. Rossi, M. Osada, J. Choi, S. Agrestini, D. Jost, Y. Lee, H. Lu, B. Y. Wang, K. Lee, A. Nag *et al.*, A broken translational symmetry state in an infinite-layer nickelate, *Nat. Phys.* **18**, 869 (2022).
- [18] L. Si, W. Xiao, J. Kaufmann, J. M. Tomczak, Y. Lu, Z. Zhong, and K. Held, Topotactic hydrogen in nickelate superconductors and akin infinite-layer oxides ABO₂, *Phys. Rev. Lett.* **124**, 166402 (2020).
- [19] See Refs. [66,67] for additional calculations showing topotactic hydrogen.
- [20] K. Lee, B. H. Goodge, D. Li, M. Osada, B. Y. Wang, Y. Cui, L. F. Kourkoutis, and H. Y. Hwang, Aspects of the synthesis of thin film superconducting infinite-layer nickelates, *APL Mater.* **8**, 041107 (2020).
- [21] Y. Cui, C. Li, Q. Li, X. Zhu, Z. Hu, Y.-f. Yang, J. Zhang, R. Yu, H.-H. Wen, and W. Yu, NMR evidence of antiferromagnetic spin fluctuations in Nd_{0.85}Sr_{0.15}NiO₂, *Chin. Phys. Lett.* **38**, 067401 (2021).
- [22] P. Puphal, V. Pomjakushin, R. A. Ortiz, S. Hammoud, M. Isobe, B. Keimer, and M. Hepting, Investigation of hydrogen incorporations in bulk infinite-layer nickelates, *Front. Phys.* **10**, 842578 (2022).
- [23] X. Ding, C. C. Tam, X. Sui, Y. Zhao, M. Xu, J. Choi, H. Leng, J. Zhang, M. Wu, H. Xiao, X. Zu, M. Garcia-Fernandez, S. Agrestini, X. Wu, Q. Wang, P. Gao, S. Li, B. Huang, K.-J. Zhou, and L. Qiao, Critical role of hydrogen for superconductivity in nickelates, *Nature (London)* **615**, 50 (2023).
- [24] A. P. Drozdov, M. I. Erements, I. A. Troyan, V. Ksenofontov, and S. I. Shylin, Conventional superconductivity at 203 Kelvin at high pressures in the sulfur hydride system, *Nature (London)* **525**, 73 (2015).
- [25] M. Einaga, M. Sakata, T. Ishikawa, K. Shimizu, M. Erements, A. P. Drozdov, I. A. Troyan, N. Hirao, and Y. Ohishi, Crystal structure of the superconducting phase of sulfur hydride, *Nat. Phys.* **12**, 835 (2016).
- [26] M. Somayazulu, M. Ahart, A. K. Mishra, Z. M. Geballe, M. Baldini, Y. Meng, V. V. Struzhkin, and R. J. Hemley, Evidence for superconductivity above 260 K in lanthanum superhydride at megabar pressures, *Phys. Rev. Lett.* **122**, 027001 (2019).
- [27] L. Boeri and G. B. Bachelet, Viewpoint: The road to room-temperature conventional superconductivity, *J. Phys.: Condens. Matter* **31**, 234002 (2019).
- [28] C. J. Pickard, I. Errea, and M. Erements, Superconducting hydrides under pressure, *Annu. Rev. Condens. Matter Phys.* **11**, 57 (2020).
- [29] Y. Nomura, M. Hirayama, T. Tadano, Y. Yoshimoto, K. Nakamura, and R. Arita, Formation of a two-dimensional single-component correlated electron system and band engineering in the nickelate superconductor NdNiO₂, *Phys. Rev. B* **100**, 205138 (2019).
- [30] L. Si, P. Worm, D. Chen, and K. Held, Topotactic hydrogen forms chains in ABO₂ nickelate superconductors, *Phys. Rev. B* **107**, 165116 (2023).
- [31] K. Lee, B. Y. Wang, M. Osada, B. H. Goodge, T. C. Wang, Y. Lee, S. Harvey, W. J. Kim, Y. Yu, C. Murthy *et al.*, Linear-in-temperature resistivity for optimally superconducting (Nd,Sr)NiO₂, *Nature (London)* **619**, 288 (2023).
- [32] P. Hohenberg and W. Kohn, Inhomogeneous electron gas, *Phys. Rev.* **136**, B864 (1964).
- [33] S. Baroni, S. de Gironcoli, A. Dal Corso, and P. Giannozzi, Phonons and related crystal properties from density-functional perturbation theory, *Rev. Mod. Phys.* **73**, 515 (2001).
- [34] D. R. Hamann, Optimized norm-conserving Vanderbilt pseudopotentials, *Phys. Rev. B* **88**, 085117 (2013).
- [35] M. J. van Setten, M. Giantomassi, E. Bousquet, M. J. Verstraete, D. R. Hamann, X. Gonze, and G.-M. Rignanese, The PseudoDojo: Training and grading a 85 element optimized norm-conserving pseudopotential table, *Comput. Phys. Commun.* **226**, 39 (2018).
- [36] K. Momma and F. Izumi, VESTA: A three-dimensional visualization system for electronic and structural analysis, *J. Appl. Crystallogr.* **41**, 653 (2008).
- [37] See Supplemental Material at <http://link.aps.org/supplemental/10.1103/PhysRevB.108.174512> for further computational details, and additional figures of the crystal structure, electronic

- structure, and phonon properties of the different phases described in the main text.
- [38] C. Heil, H. Sormann, L. Boeri, M. Aichhorn, and W. von der Linden, Accurate bare susceptibilities from full-potential *ab initio* calculations, *Phys. Rev. B* **90**, 115143 (2014).
- [39] S. Poncé, E. R. Margine, C. Verdi, and F. Giustino, EPW: Electron-phonon coupling, transport and superconducting properties using maximally localized Wannier functions, *Comput. Phys. Commun.* **209**, 116 (2016).
- [40] P. B. Allen and R. C. Dynes, Transition temperature of strongly-coupled superconductors reanalyzed, *Phys. Rev. B* **12**, 905 (1975).
- [41] C. Heil, S. Poncé, H. Lambert, M. Schlipf, E. R. Margine, and F. Giustino, Origin of superconductivity and latent charge density wave in NbS₂, *Phys. Rev. Lett.* **119**, 087003 (2017).
- [42] <https://doi.org/10.48436/zb1bp-90w68>.
- [43] W. L. McMillan, Transition temperature of strong-coupled superconductors, *Phys. Rev.* **167**, 331 (1968).
- [44] F. Giustino, M. L. Cohen, and S. G. Louie, Electron-phonon interaction using Wannier functions, *Phys. Rev. B* **76**, 165108 (2007).
- [45] P. Jiang, L. Si, Z. Liao, and Z. Zhong, Electronic structure of rare-earth infinite-layer RNiO₂ ($R = \text{La, Nd}$), *Phys. Rev. B* **100**, 201106(R) (2019).
- [46] P. Giannozzi, S. Baroni, N. Bonini, M. Calandra, R. Car, C. Cavazzoni, D. Ceresoli, G. L. Chiarotti, M. Cococcioni, and I. Dabo, QUANTUM ESPRESSO: A modular and open-source software project for quantum simulation of materials, *J. Phys.: Condens. Matter* **21**, 395502 (2009).
- [47] P. Giannozzi, O. Andreussi, T. Brumme, O. Bunau, M. B. Nardelli, M. Calandra, R. Car, C. Cavazzoni, D. Ceresoli, M. Cococcioni *et al.*, Advanced capabilities for materials modelling with Quantum Espresso, *J. Phys.: Condens. Matter* **29**, 465901 (2017).
- [48] The imaginary frequencies are plotted as negative in Fig. 3.
- [49] This calculation was performed with an in-house modified version of QUANTUM ESPRESSO. The modified code is available in accordance with the GNU license at the [42] repository.
- [50] F. Belli, T. Novoa, J. Contreras-Garcia, and I. Errea, Strong correlation between bonding network and critical temperature in hydrogen-based superconductors, *Nat. Commun.* **12**, 5381 (2021).
- [51] L. Boeri, R. Hennig, P. Hirschfeld, G. Profeta, A. Sanna, E. Zurek, W. E. Pickett, M. Amsler, R. Dias, M. I. Eremets *et al.*, The 2021 room-temperature superconductivity roadmap, *J. Phys.: Condens. Matter* **34**, 183002 (2022).
- [52] C. Heil, G. B. Bachelet, and L. Boeri, Absence of superconductivity in iron polyhydrides at high pressures, *Phys. Rev. B* **97**, 214510 (2018).
- [53] C. Heil and L. Boeri, Influence of bonding on superconductivity in high-pressure hydrides, *Phys. Rev. B* **92**, 060508(R) (2015).
- [54] W. Kohn, Image of the Fermi surface in the vibration spectrum of a metal, *Phys. Rev. Lett.* **2**, 393 (1959).
- [55] This wave vector is different from the one observed in resonant inelastic x-ray scattering (RIXS) [68,69].
- [56] F. Petocchi, V. Christiansson, F. Nilsson, F. Aryasetiawan, and P. Werner, Normal state of Nd_{1-x}Sr_xNiO₂ from self-consistent GW + EDMFT, *Phys. Rev. X* **10**, 041047 (2020).
- [57] Y. Wang, C.-J. Kang, H. Miao, and G. Kotliar, Hund's metal physics: From SrNiO₂ to LaNiO₂, *Phys. Rev. B* **102**, 161118(R) (2020).
- [58] H. LaBollita, M.-C. Jung, and A. S. Botana, Many-body electronic structure of $d^{9-\delta}$ layered nickelates, *Phys. Rev. B* **106**, 115132 (2022).
- [59] G. Pascut, L. Cosovanu, K. Haule, and K. F. Quader, Correlation-temperature phase diagram of prototypical infinite layer rare earth nickelates, *Commun. Phys.* **6**, 45 (2023).
- [60] M. Jiang, M. Berciu, and G. A. Sawatzky, Critical nature of the Ni spin state in doped NdNiO₂, *Phys. Rev. Lett.* **124**, 207004 (2020).
- [61] H. Sun, M. Huo, X. Hu, J. Li, Y. Han, L. Tang, Z. Mao, P. Yang, B. Wang, J. Cheng, D.-X. Yao, G.-M. Zhang, and M. Wang, Superconductivity near 80 Kelvin in single crystals of La₃Ni₂O₇ under pressure, *Nature (London)* **621**, 493 (2023).
- [62] V. I. Anisimov, D. Bukhvalov, and T. M. Rice, Electronic structure of possible nickelate analogs to the cuprates, *Phys. Rev. B* **59**, 7901 (1999).
- [63] J. Chaloupka and G. Khaliullin, Orbital order and possible superconductivity in LaNiO₃/LaMO₃ superlattices, *Phys. Rev. Lett.* **100**, 016404 (2008).
- [64] P. Hansmann, X. Yang, A. Toschi, G. Khaliullin, O. K. Andersen, and K. Held, Turning a nickelate Fermi surface into a cupratelike one through heterostructuring, *Phys. Rev. Lett.* **103**, 016401 (2009).
- [65] P. Hansmann, A. Toschi, X. Yang, O. K. Andersen, and K. Held, Electronic structure of nickelates: From two-dimensional heterostructures to three-dimensional bulk materials, *Phys. Rev. B* **82**, 235123 (2010).
- [66] O. I. Malyi, J. Varignon, and A. Zunger, Bulk NdNiO₂ is thermodynamically unstable with respect to decomposition while hydrogenation reduces the instability and transforms it from metal to insulator, *Phys. Rev. B* **105**, 014106 (2022).
- [67] F. Bernardini, A. Bosin, and A. Cano, Geometric effects in the infinite-layer nickelates, *Phys. Rev. Mater.* **6**, 044807 (2022).
- [68] G. Krieger, L. Martinelli, S. Zeng, L. E. Chow, K. Kummer, R. Arpaia, M. Moretti Sala, N. B. Brookes, A. Ariando, N. Viart, M. Salluzzo, G. Ghiringhelli, and D. Preziosi, Charge and spin order dichotomy in NdNiO₂ driven by the capping layer, *Phys. Rev. Lett.* **129**, 027002 (2022).
- [69] C. C. Tam, J. Choi, X. Ding, S. Agrestini, A. Nag, M. Wu, B. Huang, H. Luo, P. Gao, M. García-Fernández *et al.*, Charge density waves in infinite-layer NdNiO₂ nickelates, *Nat. Mater.* **21**, 1116 (2022).